Dalton Transactions

ROYAL SOCIETY OF CHEMISTRY

FRONTIER

View Article Online
View Journal | View Issue



Cite this: *Dalton Trans.*, 2025, **54**, 5234

# Recent advances in heavier group 15 (P, As, Sb, Bi) radical chemistry – frameworks, small molecule reactivity, and catalysis

Deana L. G. Symes and Jason D. Masuda *

Received 31st December 2024,
Accepted 25th February 2025

DOI: 10.1039/d4dt03582h

rsc.li/dalton

Main group radical chemistry has been a targeted research area for several decades. With growing examples of phosphorus radicals, even heavier pnictogen radicals including arsenic, antimony, and bismuth have also become important targets. A diverse framework of group 15 radicals has been reported in the 21st century and is covered herein. Reactivity and applications of selected radicals and future directions for this field are discussed.



## Introduction

Radical-based molecules are popular in modern chemistry but they are often unstable and short-lived due to their high reactivity. To generate and isolate main-group radicals while preventing dimerization or polymerization, these systems generally require delocalization of the unpaired electron through a π-system and the introduction of sterically hindering ligands.[1,2] The first organic radical to be isolated, $Ph_3C^{\bullet}$, was reported in 1900[3] and is stable in the solution as a free radical, but exists in the solid state as a dimer.[4] The persistence of this radical is suggested to arise from a combination of resonance contributions and steric protection from the surrounding phenyl rings.[5] Since this discovery, various radical categories have been developed including categorization by the number of unpaired electrons, electronic charge, and relative stabilities.[1]

A specific class of main group radicals that have gained popularity are phosphorus-centered radicals. These can be further divided into three general categories of neutral phosphorus radicals including phosphinyl ($R_2P^{\bullet}$), phosphonyl ($R_2PO^{\bullet}$), and phosphoranyl ($R_4P^{\bullet}$) radicals,[5,6] however, other forms such as phosphoniumyl radical cations ($(R_3P^{\bullet+})$),[7,8] carbene stabilized phosphorus radical ions (NHC) → $P^{\bullet+}(R)$,[2,9] and phosphidyl radical anions ($(R_3P^{\bullet-})$[9,10] are examples of

*Department of Chemistry, Saint Mary's University, Halifax, Nova Scotia, B3H 3C3, Canada. E-mail: jason.masuda@smu.ca*

**Deana L. G. Symes**

*Deana Symes completed her BSc with an Honours in Chemistry (2024) from Saint Mary's University with a thesis on substituted cyclopentadienyl main group complexes. Since 2024 she is pursuing an MASc at the same institution under the continued supervision of Dr Jason Masuda as an NSERC CGS-M recipient. Her research focuses on the generation and stabilization of group 15 and group 16 element-centered radicals.*

**Jason D. Masuda**

*Jason Masuda completed his BSc (2000) and MSc (2002) in Chemistry at the University of Lethbridge. After receiving his PhD in 2005 from the University of Windsor, Jason was an NSERC Postdoctoral Fellow at the University of California, Riverside and a Director's Postdoctoral Fellow at Los Alamos National Lab. He started his independent career in 2008 at Saint Mary's University and is currently a Full Professor and an Associate Dean of Science. His research is focused on ligand development/coordination chemistry, the stabilization of new main group atom combinations, and trapping highly reactive small molecules using carbenes and related molecules.*

charged phosphorus radical species that have been investigated. Nonetheless, these radicals and radical ions are arranged into three classes based on their kinetic and thermodynamic stability: stable, persistent, and fleeting or transient.[1,5,9,11] Stable radicals are long-lived, and can be isolated and stored in an inert atmosphere for extended periods without decomposing. These species are sufficiently stable to be analyzed by single crystal X-ray diffraction.[1,9,12] Persistent radicals have a shorter relative lifetime and can be characterized by standard spectroscopic methods such as electron paramagnetic resonance (EPR) or UV-vis, but cannot be isolated under standard conditions.[1,9,12] In the case of fleeting or transient radicals, these species are very short-lived due to their high reactivity and instability, resulting in unselective products, dimerization, and difficulty with characterization.[1,9]

More recently, the development of heavy group 15-based radicals including arsenic, antimony, and bismuth has begun to emerge. Examples of the heavy group 15 radical analogues are much more limited, however, there has been increased interest as of late.[13–15] The trend of increasing difficulty in radical stabilization moving down the group 15 elements can be rationalized with a few fundamental chemistry concepts. From an atomic orbital perspective, as the principle quantum number increases, the valence atomic orbitals have a larger radial extension and are more diffuse.[16] Additionally, with larger valence atomic orbitals, the energy of the highest occupied molecular orbital (HOMO) generally increases while simultaneously decreasing the energy difference between the singly occupied molecular orbital (SOMO) and the HOMO from P → Bi, making the heavier radical species easier to generate (*e.g.* milder reaction conditions or reagents). However, the heavier pnictogen-centered radical species are more reactive and therefore increasingly challenging to isolate.[17] This effect is presented throughout the literature, where a significant number of phosphorus radicals have been reported, along with many arsenic analogues,[13] however, there are a limited number of persistent or isolable antimony radicals and an even shorter list of bismuth radicals.[13,18]

The physical and chemical properties of pnictogens have a reported secondary periodicity, where an irregular change is observed throughout the group.[16,19,20] A "sawtooth" shaped pattern is observed in various electronic structure traits of pnictogens, generally arising from the large relativistic effects present in heavier atoms, and the scandide (d-block) and lanthanide (f-block) contractions of the valence shells of antimony and bismuth, respectively.[20] As previously mentioned, the valence atomic orbitals increase going down the group; however, it has a varying impact on the electronic structure, including size, pnictogen bonding, and the valence orbital ionization energy.[16] This sawtooth trend is clear when looking at the van der Waals radii of the group 15 elements, where phosphorus and arsenic radii are clustered (1.80 Å and 1.85 Å, respectively), followed by a larger jump in size to the clustered antimony and bismuth radii (2.05 Å and 2.07 Å, respectively).[16] The trend in atomic size throughout group 15 further promotes a sawtooth-like pattern with the increase in Pn–C bond lengths when comparing within the $PnPh_3$ series,[16] where the P–C (1.93 Å)[21] and As–C (1.96 Å)[22] bond lengths demonstrate a small increase but are noticeably shorter than the Sb–C (2.15 Å)[23] and Bi–C (2.25 Å)[24] bond lengths. When looking at the single electron ionization energies of the pnictogen atomic orbitals, a uniform increase of the valence p orbital energy is observed going down the group, contrarily to the s orbital ionization energy, which displays another sawtooth-like trend.[16] The energy required to remove one electron from the As 4s orbital is marginally increased compared to removing an electron from the P 3s orbital. For the heavier pnictogens Sb and Bi, a significant increase in the orbital ionization energy of the Sb 5s orbital to the bismuth 6s orbital is observed due to the significant relativistic stabilization of the latter.[16]

From the considerably impactful relativistic effects experienced by heavier elements, bismuth compounds have distinctive properties compared to their lighter pnictogen congeners (N, P, As, Sb), such as the inert pair effect observed for the $6s^2$ electron pair which remains formally unoxidized, however, can be stereochemically active.[14,24–28] Relativistic effects are responsible for or influence certain properties of heavy elements such as their colour, the geometries of heavy element-containing molecules, and their reactivity behaviour.[24] When looking at the s and p orbitals going down the group 15 elements, there is a significant decrease in the spatial overlap of the 6s and 6p orbitals due to their increasing size difference, resulting in less s/p mixing to give essentially non-hybridized orbitals for bismuth.[14,16] With the large and diffuse atomic orbitals of bismuth, this leads to inefficient overlap with the orbitals of other bound atoms, resulting in weaker and longer Bi–E bonds.[14,16,29] This effect has been observed with the Pn–H bond dissociation enthalpies for the $PnH_3$ series (Pn = P: 81.4; As: 74.6; Sb: 63.3; Bi: 51.8 kcal $mol^{-1}$),[30,31] where the valence *s*-character of the heavier elements going down the group tends to accumulate in a non-bonding lone pair type orbital. This leads to the Pn–H bonds being made essentially by unhybridized p-orbitals.[14,16,32]

In the 21st century, there are a few reviews on the recent developments of pnictogen-centered radicals.[1,5,9,10,13,18,33] Additional reviews in the literature describe specific areas of group 15 radical chemistry including the use of carbene ligands for effective stabilization,[2,34] synthesis and reactivity of biradicals,[35] as well as the applications of EPR spectroscopy[36] and frustrated radical pairs.[37,38] group 15 radical species possess the potential for stoichiometric and catalytic transformations including small molecule activation and conversion, as well as thermal and photochemical coupling reactions, which are areas that transition metals have otherwise dominated. Herein, we aim to highlight recent developments within group 15-based radicals and the direction we envision as the next potential steps moving forward in new and related research. Our goal is to contextualize the significance of these developments and discuss the challenges still faced in the area of group 15-based radicals while putting this area in a new perspective.

## Phosphorus-centered radicals

### Phosphinyl radicals

Phosphinyl radicals are neutral two-coordinate radicals with an unpaired electron and a lone pair, commonly generated by homolytic cleavage of a P–P single bond.[9,39–41] The homolytic bond dissociation of P–P bonds is generally a non-spontaneous process, with the parent diphosphine, $H_2P$–$PH_2$ having a bond dissociation energy (BDE) of 61.2 kcal $mol^{-1}$.[42,43] Although this energy barrier is much lower than its carbon analogue, it remains sufficiently high, preventing the homolytic cleavage of the P–P bond.[42,44] This facile dimerization can create challenges in the utility of these phosphorus radicals, necessitating the development of an approach to stabilize these species. By tuning the steric and electronic properties of the substituents, homolytic cleavage of the P–P bond is encouraged in solution through steric crowding of the radical center, which elongates and weakens the central P–P bond. Additionally, dimerization can be minimized through the resonance stabilization of the unpaired electron by delocalization through a conjugated system.[42,45–47]

Other factors that determine the dissociation equilibrium are the system's dispersion forces and entropic effects. When dispersion forces are neglected, it is calculated that many diphosphanes would be energetically more favourable as their respective monomeric radical species in the solid state rather than their dimeric forms.[48] Since this is not the case for experimentally observed results,[17,39–41,45,47,49–52] it reinforces the significance of dispersion force effects in the theoretical calculations of sterically crowded molecules.[48] Increased steric bulk of the substituents gives rise to an increase in strain energies and steric repulsion between the substituents, thus the attractive dispersion forces prevail over the susceptibility of the dimer to dissociate.[48]

Methods for generating diphosphines that homolytically cleave to give phosphinyl radicals, or the direct formation of phosphinyl radicals typically involve the reduction of $R_2P$-X (X = halide). Generally this is done with common reducing reagents such as magnesium metal,[51,53] potassium on graphite,[1,54,55] or metallocences such as $[Cp_2TiCl]_2$ and $[Cp_2Ti(btmsa)]$ (btmsa = bis(trimethylsilyl)acetylene).[53] In other approaches, one electron oxidation of an amino phosphalkene[56] or a cationic phosphanide[57] and reduction of a fluorenyl-based phosphalkenes with potassium or lithium metal[58] are a few additional redox approaches for generating phosphinyl radicals. Other phosphinyl radical generating processes include photochemical dehydrocoupling of N-heterocyclic phosphanes to form the related diphosphines that can homolytically cleave to form the radical[59–61] as well as thermochemical generation in the presence of radical initiators.[62]

Two popular frameworks for phosphinyl radicals are the dialkyl-substituted and the bis-amido-phosphorus derivatives. The first report on persistent phosphinyl radicals was published in 1976 by Lappert *et al.*,[49] where a radical for each framework was generated (**1a–b**), containing bis(trimethylsilyl) groups on the atoms adjacent to the phosphorus center (Scheme 1).[49] The substantial steric strain of these bulky substituents accumulates significant potential energy, which induces the parent diphosphines to dissociate into the respective phosphinyl radicals when released from the solid state.[47–50,63] This specific design is known in the literature as a molecular "jack-in-the-box" as the substituents behave similarly to stored energy in a compressed spring.[47,48,63]

Furthermore, the substituents adjacent to the phosphorus radical center can easily be modified to explore an array of steric environments. Many examples have been described in the literature including diphosphines incapable of homolytic cleavage (**2**),[64] persistent asymmetric acyclic (**3–7g**),[50,65–67] and symmetric acyclic (**7h**)[66] or cyclic (**8–11**)[17,40,41,45,51,52,55] radicals in the solution state (Fig. 1). Although **2** contains a bulkier backbone than **9–11**, this species does not dissociate into the monomeric radical form as the isopropyl substituents have minimal steric repulsion.[64] The examples **3–10** are dimeric in the solid state, however, in solution, they exist in an equilibrium between the diphosphine and the phosphinyl monomer, which gives radical character when in solution. Compound **11** was the first example of a phosphinyl monomer in the solid state.[55] Compounds **8a–c** contain a unique phosphinyl radical framework where a ferrocene fragment is incorporated into the structure by linking it to the terminal heteroatoms (P or N) in the P–P–P and N–P–N systems, providing a rigid cyclic structure beneficial for selective stereochemistry.[52]

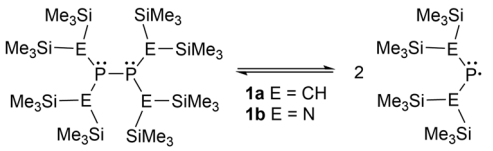


**Scheme 1** Equilibrium of the diphosphine and its respective phosphinyl radical in solution.

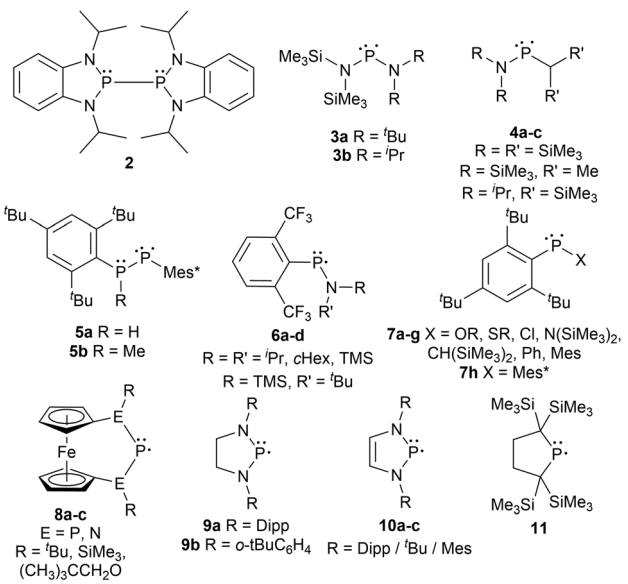


**Fig. 1** A diphospine (**2**) and phosphinyl radicals (**3–11**).

### Phosphorus-centered radical ions

In the literature, there are both phosphorus radical cations and phosphorus radical anions, with the former being more prevalent (Fig. 2).[1,33] Although this observation has been addressed in the literature,[1,33] the underlying reasons were left to the reader's interpretation. When comparing a phosphorus radical cation to a phosphorus radical anion, the former has an overall positive charge, making the unpaired electron less susceptible to reactivity as it is held more tightly by the phosphorus radical center. Additionally, most phosphorus radical ions are generated from P(III) species, where the resulting radical ion has two or three substituents: in many cases, carbon-based groups. These substituents inductively donate electron density to the radical center, stabilizing cationic species but de-stabilizing anionic species, making them more challenging to isolate.

The generation of stable phosphorus radical cations continues to develop by incorporating sterically bulky substituents allowing for the delocalization of the positive charge across a larger area.[10,33] These radical species are typically generated by reducing phosphorus-containing unsaturated bonds, such as those found in phosphalkenes[10,33] or diphosphenes,[68,69] with strong reducing agents such as alkali metals.

Phosphorus radical cation examples in the literature generally consist of tricoordinate aryl-substituted phosphorus radical centers (**12**),[7,8,70] or 4-membered ring systems of dimeric phosphorus species; $N_2P_2$ (**13**, **14a**),[71,72] $C_2P_2$ (**14b**)[73] $P_2P_2$ (**14c**),[71] and $Ge_2P_2$ (**15**).[74] Other examples of phosphorus radical cations are those containing phosphaalkenes (**16**, **17**),[75] a tetraaryldiphosphine (**18**),[76] and diphosphadibenzo[*a*,*e*]pentalenes (**19a–b**) (Fig. 2).[77] For phosphorus radical anions, the examples are more limited, however, they contain dicoordinate aryl-substituted diphosphenes (**20a–c**),[68,69] boryl-substituted diphosphenes (**20d**),[78] phosphaalkenes (**21–24**),[79–83] and the rigid chelating diamidodihydroacridinide ligand (**25**), where the radical precursor contains a vacant p-orbital suitable as an acceptor orbital for one electron reduction reactions (Fig. 2).[84] Many of these radical ionic species have been previously discussed in detail in recent review-type articles.[9,10]

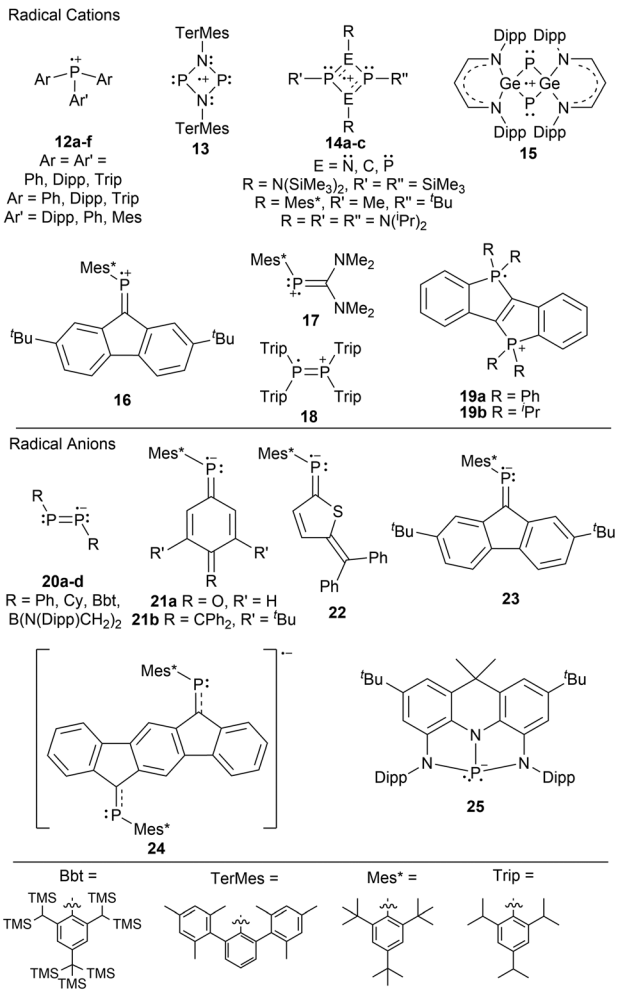


Fig. 2 Phosphorus radical cations and radical anions.

### Carbene stabilized phosphorus radicals

Innovative designs for stabilizing radicals are often used and over the last two decades, singlet carbenes have proven their utility in this manner.[82,85–92] The use of N-heterocyclic carbenes (NHCs) and cyclic(alkyl)(amino) carbenes (CAACs) has allowed for the generation, and occasionally the isolation of radical-containing species, which otherwise could not be detected spectroscopically.[2] Carbenes effectively stabilize inherently highly energetic radical centers due to their tunable, typically bulky substituents, and a low-lying empty carbon p-orbital available to accept and delocalize electron density of the unpaired electron.[85,93–95] A minireview of carbene stabilized main group radicals and radical ions was published[2] in 2013 and includes pnictogen-centered derivatives, however, additional carbene-stabilized pnictogen-based radicals have since been reported.[87,88,90,90–92]

There are a few variations of phosphorus-centered radicals and radical ions stabilized by carbenes including single phosphorus atoms (**26**, **27**),[56,57] phosphorus-phosphorus systems (**28a–c**),[87,89] nitrogen–phosphorus systems (**29**),[96] and systems containing multiple nitrogen and or multiple phosphorus atoms N–P–N (**30a**),[97] P–P–P (**30b**),[98] P–N–P (**31**),[91] and P–N–P–N (**32a–b**)[92] (Fig. 3). In most cases, the species generated is a radical cation[56,87,89,92,96] or a radical dication,[57] except for the neutral tripnictogen systems,[91,97,98] or in a more recent development that includes a neutral diphosphene radical stabilized by a carbene and a Dipp group (**33**).[90] Other radicals incorporating a carbene functionality include a diphosphene stabilized by an N-heterocyclic vinyl (NHV) scaffold (**34**),[88] dicarbondiphosphide-based radical cations stabilized by NHCs (**35**, **36**),[99,100] and an α-radical phosphine species (**37**)[101] generated by reducing a bicyclic(alkyl)(amino)carbene (BICAAC) stabilized phosphenium cation (Fig. 3).

Fig. 3 shows that these radical systems can also be categorized by whether they contain two identical or different NHCs, two CAACs, one NHC and one CAAC, or a single CAAC. When comparing five-membered NHCs with saturated or unsaturated back-

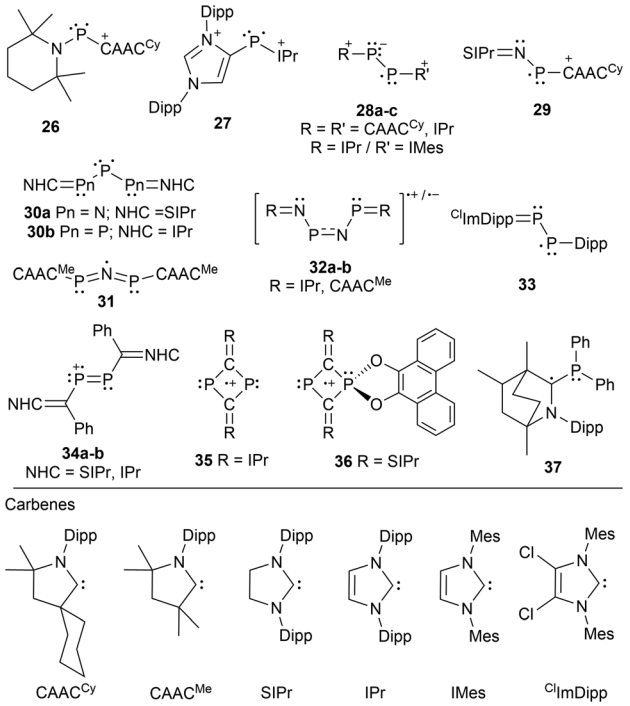


Fig. 3 Carbene stabilized phosphorus and phosphorus–nitrogen based radicals.

bones, the former is typically calculated to be the stronger σ-donor and stronger π-acceptor. However, when considering CAACs the σ-donor and π-acceptor properties are further strengthened, making CAACs a better choice for radical stabilization.[102] This difference in donor and acceptor abilities can be recognized as a consequence of the energy difference between the highest occupied molecular orbital (HOMO) and the lowest occupied molecular orbital (LUMO), where the HOMO-LUMO gap of an NHC is typically larger compared to those of CAACs.[102,103]

# Heavy group 15 based radicals

### Arsenic-centered radicals

The first arsenic paramagnetic species to be structurally characterized in the solid state was an arsenic radical cation stabilized by two NHCs in 2013 (**38**).[104] Only a few years after this initial discovery, a minireview on long-lived heavier Group 15 radicals was published[13] in 2020, listing a variety of arsenic-centered radicals. Similar to the frameworks listed for phosphorus-centered radicals, arsenic derivatives of dicoordinate bis-trimethyl silyl substituted acyclic[49,50] and cyclic[17] neutral radicals (**39**, **40**), tricoordinate aryl-substituted radical cations (**41**),[105] tricoordinate tris-amide substituted radical anions (**42**),[84] tripnictogen-centered radicals (P–As–P) stabilized by two NHCs (**43**),[98] radical dications stabilized by two CAACs (**44**),[106] and dicoordinate organoarsenic radical anions (**45**, **46a**)[107] and biradical dianions (**46b**, **47**)[107] have been reviewed (Fig. 4).[13]

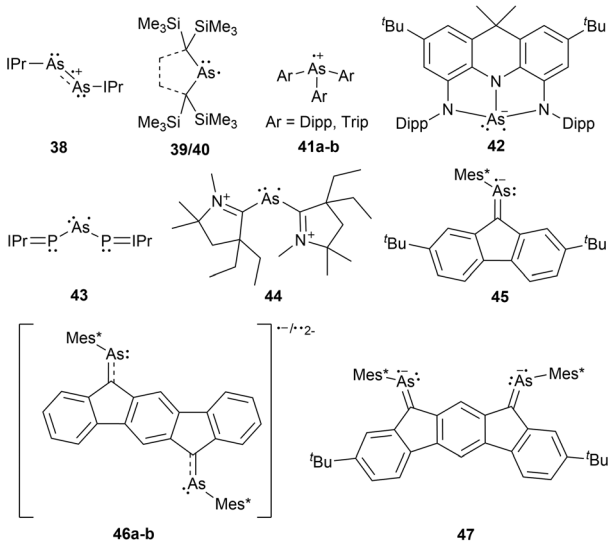


Fig. 4 Arsenic-centered radical analogues of phosphorus-based systems.

Newer radical systems have also been reported for arsenic radical derivatives where some have been previously discussed in reviews.[108] Phosphaarsene (P–As) radical cations (**48**)[109] and radical anions (**49**)[110] stabilized by carbenes and aryl groups respectively have been generated, with the former being isolated. There have also been reports of dicoordinate radical cations stabilized by a single CAAC, where the other coordinating group is an NHV scaffold (**50**),[111] and radical cations within 4-membered ring systems of arsenic dimers, $As_2N_2$ (**51a**),[72] and mixed pnictogens, AsNPN (**51b**).[72] The newer systems not covered by previous reviews include dicoordinate radical cations stabilized by a CAAC and a gallium substituent (**52**),[112] or arsenic radical centers stabilized by two gallium substituents (**53**)[113] (Fig. 5).

### Antimony and bismuth-centered radicals

The heavy pnictogen-centered radicals of antimony and bismuth have limited examples in the literature. As mentioned in the introduction, the list of persistent or isolable bismuth radicals has significantly fewer examples than that for anti-

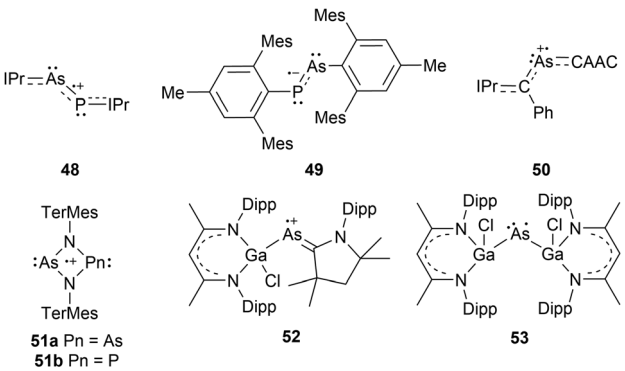


Fig. 5 Arsenic-centered radicals generated with new frameworks.

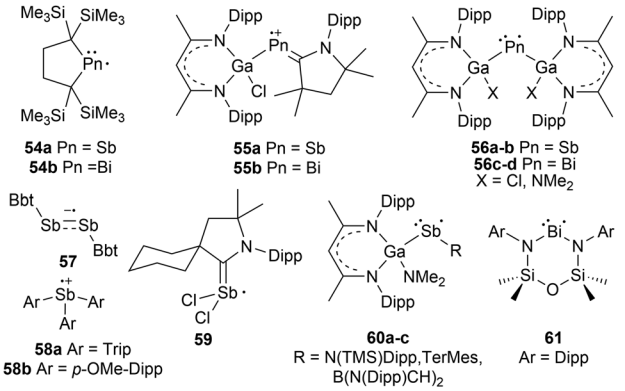


**Fig. 6** Antimony and bismuth-centered radicals described in the literature.

mony, which may be attributed to the higher tendency for bismuth radicals to undergo decomposition and dimerization reactions.[13,18] Nonetheless, these radicals can be generated under a few conditions similarly to phosphorus-centered derivatives. The homolytic cleavage of dipnictogen bonds[17,114] or Pn–E bonds (E = C, O, transition metal fragment)[29,115–120] in reversible equilibrium reactions[114] or non-reversible conditions[115] respectively is a standard strategy that employs mild reaction conditions for the generation of some antimony and bismuth radicals.[18] Similarly, methods including photochemically induced homolytic bond dissociation have been investigated for these pnictogens, with no success in isolating the radical species generated, however, their implementation as radical intermediates in stoichiometric and catalytic reactions has been reported.[15]

As anticipated, analogues to the phosphorus and arsenic radicals previously discussed have been generated for antimony and bismuth. These include dicoordinate bis-trimethylsilyl substituted neutral radicals (**54a–b**),[114] dicoordinate radical cations stabilized by a single CAAC and a gallium-based substituent (**55a–b**),[112] and bis-gallium-based substituted neutral radicals (**56a–d**)[113,121,122] (Fig. 6). Unlike the phosphorus and arsenic analogues, the stibinyl and bismuthinyl radicals **54a** and **54b** are reported as dimers in the solid state.[17] With the small covalent radii of phosphorus and arsenic relative to antimony and bismuth, the lighter pnictogens are more sensitive to steric influences, in this case, the steric repulsion of the bulky trimethylsilyl substituents.[16,17] The influence of changing the pnictogen radical center from phosphorus to bismuth is displayed by the varying Pn–C bond lengths and C–Pn–C bond angles throughout this series (Table 1).

For antimony, this list can be expanded to include a dicoordinate aryl substituted distibene radical anion (**57**),[69,121] triarylstibine radical cations (**58a–b**),[123] and a carbene-stabilized neutral dichlorostibanyl radical (**59**);[124] the first antimony-centered radical to be characterized in solution. In addition to the pre-existing systems, some systems have been altered to generate unique antimony and bismuth radicals. New radical systems incorporating a gallium-based substituent and either an amine (**60a**), aryl group (**60b**), or N-heterocyclic borane (**60c**) have been explored for antimony.[116] For unique bismuth radicals, a diamidobismuth(II) radical has been isolated and characterized (**61**) (Fig. 6).[125]

Another example of trends descending through Group 15 is the tricoordinate aryl-substituted radical cations. For the $[Trip_3Pn]^{\bullet+}$ (Pn = P, As, Sb) series, a decreasing trend in the sum of the C–Pn–C bond angles has been reported going down the group (359.99° (P),[8,105] 354.35° (As),[105,126] 348.54° (Sb)[123,126]). As a comparison, for the neutral and sterically comparable $Dipp_3Pn$ series the sum of the C–Pn–C bond angles also decreases from P to Bi 335.01° (P),[70,127] 328.83° (As),[127,128] 320.88° (Sb),[127] 318.50° (Bi).[129] The phosphorus radical cation species is planar, whereas a slight pyramidalization is observed for the arsenic and antimony derivatives. The structural differences observed in this series can be rationalized by the increase in atomic radius going down the group, creating longer Pn–C bond lengths and a reduced degree of steric shielding from the bulky substituents.[8,105,123]

## Biradicals

Biradicals are an even-electron molecular species containing two radical centers in two degenerate (or nearly degenerate)

**Table 1** Experimental and calculated bond lengths (Å) and angles (°) for a series of P to Bi radicals

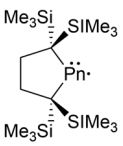


| Pn | P | As | Sb[b] | Bi[b] |
|---|---|---|---|---|
| Pn–C X-ray | 1.869(1) | 2.006(2), 2.007(2) | 2.252(2) | 2.371(3), 2.370(3) |
| C–Pn–C X-ray | 96.16(5) | 92.98(7) | 86.92(7) | 84.74(9) |
| Pn–C calc[a] | 1.877, 1.878 | 2.005 | 2.217, 2.218 | 2.318, 2.323 |
| C–Pn–C calc[a] | 95.120 | 91.816 | 86.557 | 84.131 |

[a] Optimized at (U)M06-2X/def2-SVP level of theory. [b] X-ray bond lengths and angles are from the Pn–Pn dimer.

orbitals that are nearly independent of each other.[35,53,130–133] In terms of biradicaloids, this refers to biradicals in which the two radical centers interact significantly.[35,134,135] These two systems can be further differentiated by the spin of the two unpaired electrons. For biradicals, the spin of the two electrons is parallel, resulting in a triplet state, whereas in biradicaloids, the spin of the two electrons is antiparallel, forming an open-shell singlet state.[53,130,132] Furthermore, another type of biradical includes disbiradicals, which are biradicals that display negligibly small to no coupling between the two unpaired electrons and give, in spectroscopic terms, two-doublet radical species.[35,131,132,135] For simplicity, since there is no defined measurable degree of interaction, the term biradical is used synonymously for biradicaloid in this review, as similarly done in previous publications.[35,135]

Heteroatom-based biradical systems have recently been extensively reviewed by Schulz,[135] as well as a more specific Frontier article on cyclobutane-1,3-diyl and cyclopentane1,3-diyl group 15 biradical analogues by Schulz and coworkers.[35] To avoid significant repetition of this work, a brief background of biradicals and some highlights of group 15 biradicals will be discussed, followed by an overview of newer developments within this field. To begin, after Gomberg reported the trityl radical as the first observed organic radical species in 1900[3] the report of the first biradical **62** was published by Schlenk and Brauns in 1915.[136] This biradical species was generated by the reduction of two C–Cl bonds of 1,3-(diphenylchloro)phenyl with copper bronze (CuSn) (Scheme 2).[136] Studies of heteroatom-containing biradicals were initiated by the study of the four-membered sulfur-nitrogen heterocycle $S_2N_2$ (**63**)[137] and later were reinvigorated by the Niecke-type biradicals (**64**) (Scheme 2).[138,139]

In-depth studies of the $P_2C_2$ heterocyclic system, 1,3-diphospha-cyclobutane-2,4-diyl, have been done by the Niecke group[138] as reviewed by Schoeller[139] which facilitated the experimental and theoretical investigations of cyclobutane1,3-diyl analogues of the type $[E(\mu NTerMes)E']_2$ (E = E′ = P, As, Sb, Bi; E = P, E′ = As)[130,140–142] (**65a–e**) (Scheme 3). For the biradicals **65a–e**, the phosphorus and arsenic derivatives have been reported in good yields, however, the heavy analogues, antimony and bismuth, have only been observed *in situ* due to their higher relative reactivity.[135] Based on theoretical calculations, when going down group 15 (P → Bi) the biradical character significantly increases in the $[E(\mu NTerMes)E']_2$ (E = E′ = P, As, Sb, Bi) series as observed in the elongation of the *trans*-annular E–E′ distances in a sawtooth-like pattern (E = E′ = P: 2.669 Å; As: 2.896 Å; Sb: 3.250 Å, Bi: 3.386 Å).[130,140,141]

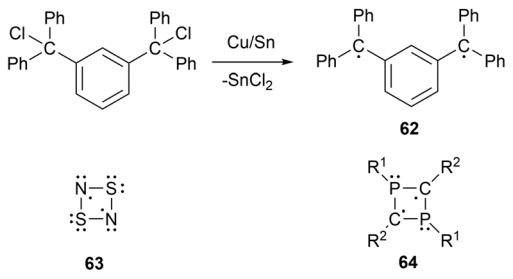


**62** **63** **64**

Scheme 2 Pioneering research for main group biradicals.

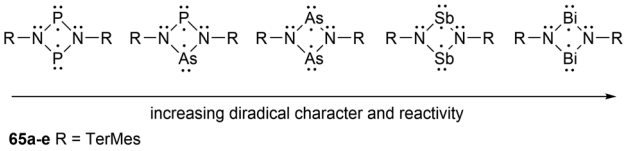


**65a-e** R = TerMes

Scheme 3 Altering properties in four-membered biradical ring systems by changing the pnictogen atom(s).

For newer developments in this field, improvements in the synthesis of four-membered cyclic biradical systems (**66**) have been recently reported from the reduction of acyclic materials[134] alternatively to the classic reduction of the halogenated heterocyclic precursors (Scheme 4).[35] Additionally, as theorized in the review by Hinz *et al.*[135] the first phosphorus-centered dis-biradical, linked by a hexyl ligand was synthesized (**67**).[132] Recently as well, Schulz *et al.* reported a zirconocene-bridged phosphorus-centered bis-biradical (**68**), the first bis-biradical-based molecular switch attached to a transition metal fragment (Fig. 7).[143] Additionally, in 2023, monocoordinated antimony and bismuth complexes in a triplet ground state were isolated incorporating sterically demanding hydrindacene-based ligands to obtain a stibinidene (**69**)[144] and bismuthinidene (**70**).[145] Further discussion of these species or analogous derivatives can be found in a later section; light-induced reactivity.

## Radical reactivity studies

### Radical coupling reactions

Main group element-centered radicals are highly chemically reactive species due to the presence of an unpaired electron.[10,108] Historically, these species undergo poorly controlled reactions, however, this research field is rapidly developing with their importance in theoretical, biological, and synthetic chemistry, as well as material science.[1,10,108] The utilization of sterically encumbering substituents to create kinetic[2,10,108] and thermodynamic barriers[146] and π-conjugated systems to delocalize the unpaired electron density are applied strategies to stabilize radical-containing species.

Cross-radical coupling reactions are a frequently performed reactivity experiment that supports the generation of a radical

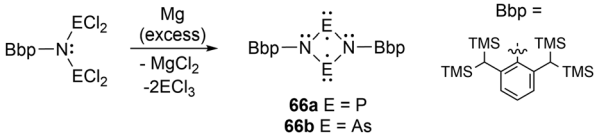


**66a** E = P
**66b** E = As

Scheme 4 Reduction acyclic materials to generate four-membered cyclic biradicals.

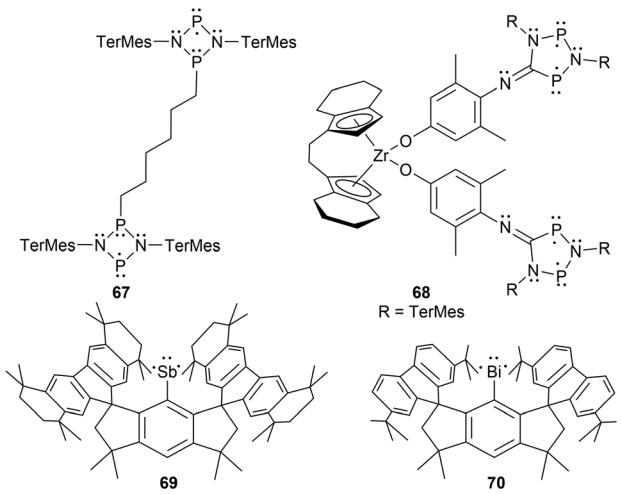


Fig. 7 Recent developments of multi-radical centered pnictogens.

species. A cross-radical coupling reaction involves the combination of two radicals to generate a new bond, which can capture the radical species of interest in a more stable form. A readily available reagent used in many cases is 2,2,6,6-tetramethylpiperidine-1-oxyl (TEMPO). Cross-radical coupling products of TEMPO with the pnictogens discussed in this paper have been reported in various studies.[17,39,114,147] Another reagent investigated for cross-radical coupling reactions is 2-azaadamantane-*N*-oxyl (AZADO), another stable aminoxyl radical.[39] When the phosphinyl radical **11** is reacted with TEMPO, the rearrangement product **71** is observed, however, when reacted with AZADO, three rearrangement products are observed (**71**, **72**, **73**). The heavier pnictogen radical analogues (**40**, **54a**, and **54b**), have been investigated in radical cross-coupling reactions with TEMPO, yielding the anticipated cross-coupling products (**74a–c**) (Fig. 8).[17] Another unique phosphorus-centered radical system investigated in similar radical trapping reactions includes a square pyramidal phosphoranyl radical.[148] This radical is very unstable and readily dimerizes, however could be trapped with benzophenone and $(C_6F_5)_2CO$ as radical adducts (**75a–b**) (Fig. 8).[148]

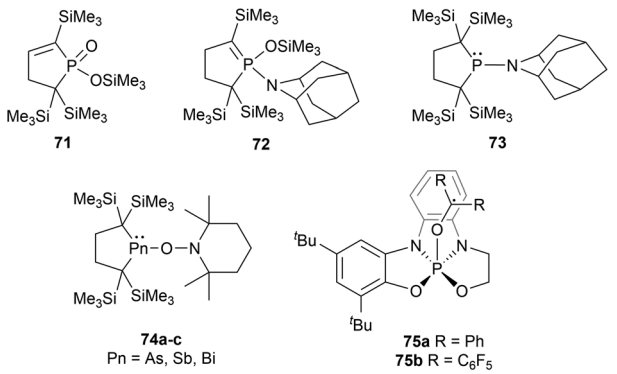


Fig. 8 Radical cross-coupling products for group 15 radicals.

The reaction of the stable phosphinyl radical **11** with AZADO generated the anticipated radical coupling product **76** at −40 °C as an intermediate species.[39] When warmed to room temperature, the aminoxyphosphine **76** decomposes to the silyl phosphinate **71**, the cyclic phosphorane **72**, and the aminophosphine **73** in 7%, 82%, and 5% yields, respectively, with the remaining trace amounts being unidentified products. This distribution of products is drastically changed when the reaction is conducted at room temperature, giving a more even distribution of 27% (**71**), 28% (**72**), and 35% (**73**).[39] Based on the products observed for the decomposition of the aminoxyphopshine intermediate **76**, a proposed mechanism was suggested by Iwamoto *et al.*, as seen in Scheme 5.[39] The first suspected step of this mechanism involves the homolytic cleavage of the N–O bond to give the aminyl (**77**) and phosphinoyl (**78**) radicals, where the latter radical intermediate (**78**) undergoes a 1,3-silyl migration to generate the more energetically favourable radical **77**. Next, there are three variations of radical coupling reactions as seen in Scheme 5 that give **72**, **73**, and **80**. To generate the third observed product **71**, a second N–O bond cleavage of **80** followed by hydrogen abstraction is the suggested formation mechanism.[39]

For the arsenic cross-coupling product **74a**, two sets of signals were observed by EPR spectroscopy, suggesting a partially reversible dissociation of the product into the arsinyl radical **40** and TEMPO due to the shorter Pn–O bond distance, causing severe steric hindrance between the two subunits. For the antimony derivative, the Pn–O bond is longer, slightly reducing the steric strain, and therefore does not dissociate into the stibinyl radical **54a** and TEMPO.[17] This concept is further supported by the molecular structures of the cross-coupling products **74a** and **74b**, as the intramolecular distances of the methyl carbons of the trimethylsilyl substituents and TEMPO have a shorter average bond distance in the arsenic derivative (3.77 Å) compared to that observed in the antimony derivative (3.91 Å).[17] Despite the longer Pn–O bond for the bismuth derivative **74c**, which would further reduce the steric repulsion between the bulky alkyl ligand and TEMPO moieties, this cross-coupling product reversibly dissociates to

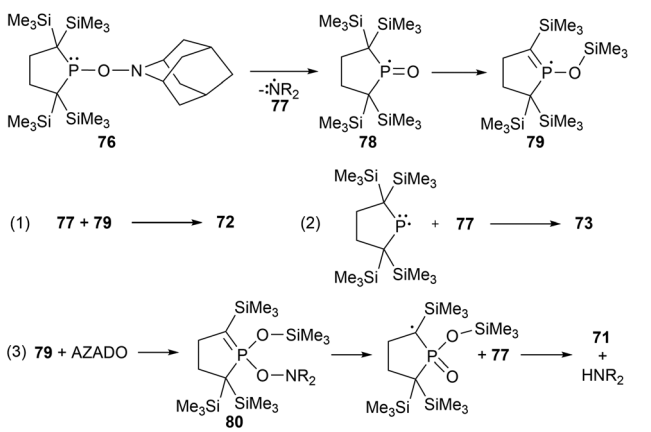


Scheme 5 Proposed formation mechanism for **71–73**.

the bismuthinyl radical and TEMPO. With significantly large and diffuse orbitals on bismuth, it is predicted that this reported observation is due to the weak Bi–O bond.[17]

### Small molecule reactivity

A few of the Group 15 radicals listed have been investigated within small molecule reactivity studies. The phosphinyl radicals **1a** and **9a** have been investigated by adding various chalcogens ($O_2$, $S_8$, Se, and Te), resulting in chalcogen-bridged diphosphines (Scheme 6).[45,149] In a subsequent report, **9a** was reacted with carbon disulfide, phenyl isocyanate, and phenyl isothiocyanate.[41] The radical species were added across the C=S and C=O double bond to generate neutral diamagnetic species.[41] Similar reactivity of 4-membered cyclic phosphorus (**64a**) and arsenic (**64c**) biradicals were also reported (Scheme 6).[35,53,140,150,151]

Phosphorus radicals **3b**,[67] **9a**,[45] and **33**[90] have also been used for white phosphorus ($P_4$) activation. In all cases, a butterfly-type core structure was observed, capped by two of the phosphorus radical fragments (Scheme 7).[45,90] Further reactivity of radicals **9a** and **33** was attempted with other small molecules including $CO_2$, CO, and $H_2$ however no reactions were observed. In other work, a tetraradical (**81**) made by Schulz *et al.*, was successfully applied in the activation of two equivalents of $H_2$ (Scheme 7).[131]

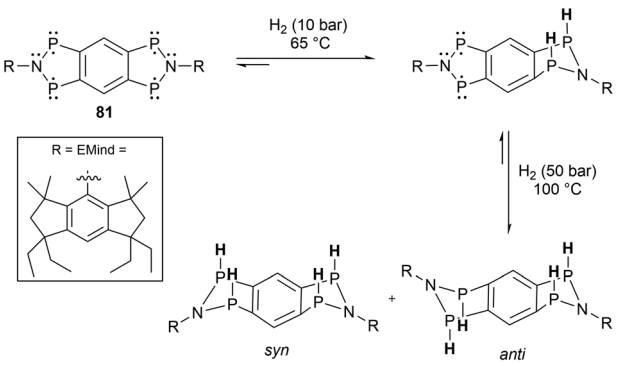


**Scheme 7** $H_2$ activation by the tetraradical (**81**).

For biradicals, the four-membered ring system [P(μNTerMes)]$_2$ (**64a**) has undergone reactivity with CO, where the CO inserts into a P–N bond to generate the hetero cyclopentane-1,3-diyl biradical **82**, which was subsequentially reacted with various small molecules (Scheme 8).[152] Following this work, the four-membered biradical ring systems **64a** and **64b** were reacted with isonitriles CN-R′ (R′ = N(SiMe$_3$)$_2$, $^t$Bu, TerMes, DMP = 2,6-dimethylphenyl, and Mtp = 2,6-dimethyl-4-tert-butyl-phenyl) to generate new cyclopentane-1,3-diyl derivatives, **83a–d**, and **84a–d**, respectively, by once again, inserting the carbon atom into a P–N bond (Scheme 9).[153,154] The biradicals **83d**, was then further reacted in a later study by Schulz *et al.* to generate Staudinger-type adducts **85a–b**.[155]

### Light-induced reactivity

More recently, phosphorus-based radicals have been implicated in light-induced reactivity studies. The bimetallic Ni complex **86**, was investigated with bond activation reactions using visible light, indicating that the diphosphine P–P bond behaves as an active site under these conditions, demonstrating radical-type reactivity.[156] By irradiation with 536 nm light, a variety of bonds including H–H, N–H, N–N, and O–H were

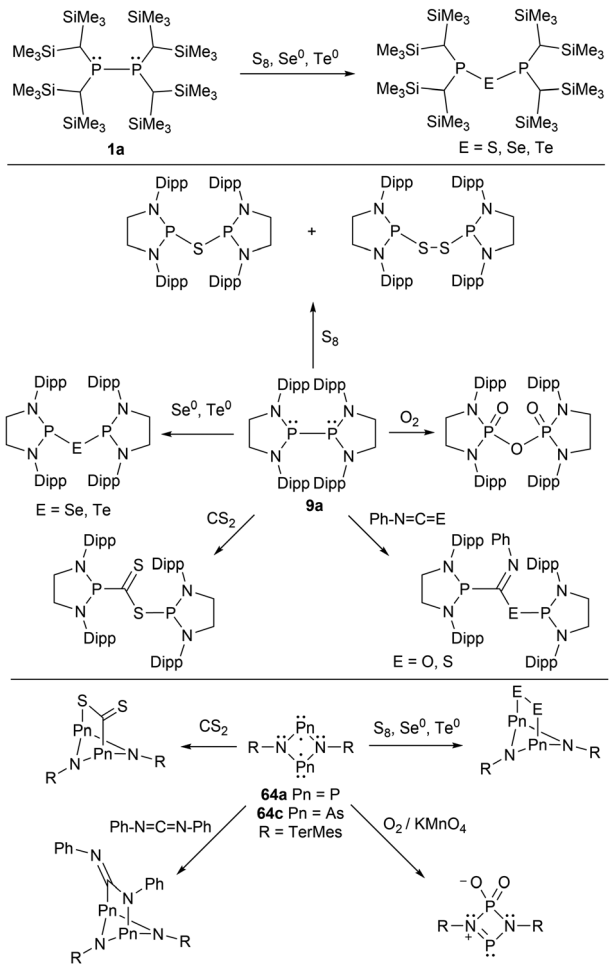


**Scheme 6** Reactivity of phosphinyl radicals (**1a**, **9a**) and biradicals (**64a**, **64c**) with chalcogens and other small molecules.

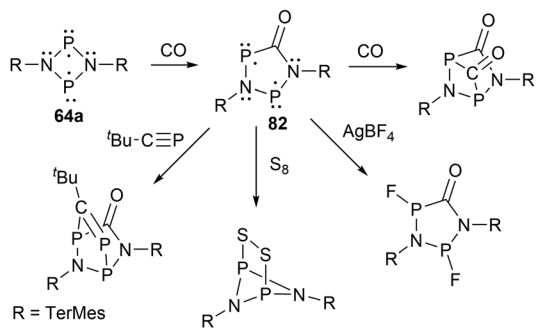


**Scheme 8** Generation of cyclopentane-1,3-diyl biradical **82** and its reactivity studies.

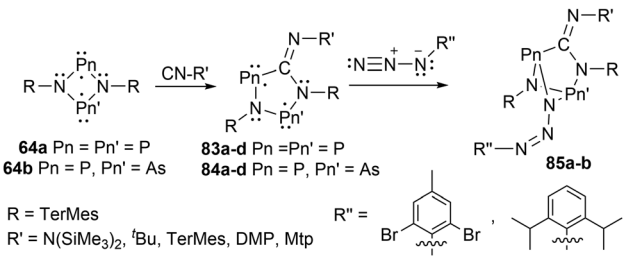


**Scheme 9** Reactivity of biradicals of the type [E(μNTerMes)E']$_2$ to generate cyclopentane-1,3-diyl derivatives (**83a–d**, **84a–d**), and Staudinger-type adducts (**85a–b**).

activated by the light-induced cleavage of the P–P bond of **86** (Scheme 10).[156] Another study reported light-induced functionalization of diazaphospholenes with electrophiles *via* the phosphinyl radical **10b** in the absence of radical initiators at room temperature (Scheme 11).[157] The two products generated in these reactions could then easily be separated by their solubilities.[157]

Furthermore, in the recent literature, diazaphospholene-catalyzed radical reactions have been reported.[60,61] Diazaphospholene-mediated cyclization of aryl halides was earlier reported using stoichiometric amounts at room temperature [Scheme 12, eqn (1)],[157] followed by radical intramolecular annulations of aryl halides with stoichiometric diazaphosphinane at elevated temperatures in the presence of the radical initiator azobis(isobutyronitrile) (AIBN) [Scheme 12, eqn (2)].[62] In this work it is suspected that the phosphinyl radical

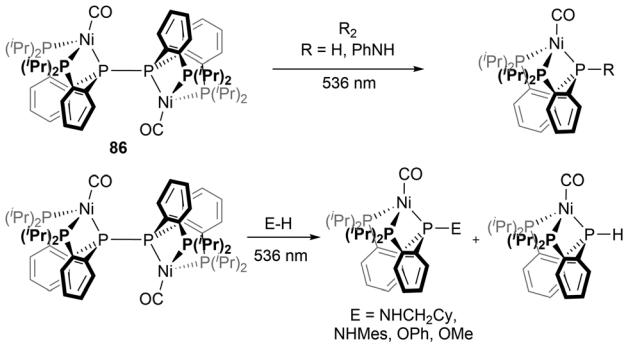


**Scheme 10** Photo-induced P–P bond cleavage of a rare metal-based diphosphine and reactions with small molecules.

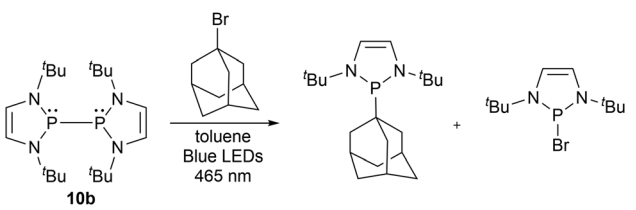


**Scheme 11** A selected example of photoinduced P–P bond cleavage and activation of an sp$^3$ hybridized C–Br bond.

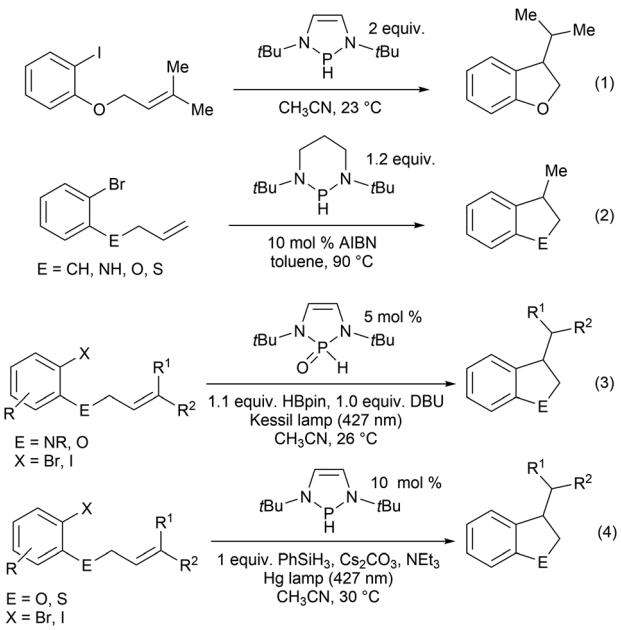


**Scheme 12** Stoichiometric and catalytic ring closure reactions that implicate phosphorus-based radicals as an active species in the reaction.

generated activates the carbon–halogen bond through a mechanism involving single electron transfer (SET).[62,157] In 2022, the introduction of visible light irradiation significantly accelerated the annulation of aryl halides and requires as little as 5% mol catalyst loading of the phosphine pre-catalyst in a DBU/HBpin system [Scheme 12, eqn (3)][61] and 10% mol catalyst loading phosphine pre-catalyst when combined with phenylsilane, an alkali metal salt, and a base [Scheme 12, eqn (4)].[60]

The proposed catalytic cycles for the cyclization of aryl halides previously discussed (Scheme 12; eqn (3) and (4)) have been reported and feature equivalent key intermediates.[60,61] In both cases, a pre-catalyst is introduced to the system and converted to the respective phosphinyl radical by light irradiation at 427 nm. However, for Cramer's approach, an additional step of reducing the phosphine oxide with HBpin must be done prior. The generation of the phosphinyl radicals initiates a radical chain process by abstracting the halide, resulting in the aryl radical (**I**) and a phosphine halide.[60,61] The aryl radical then adds across the C=C bond in a 5-*exo*-trig manner to generate an alkyl radical (**II**). Separately, the phosphine halide reacts with HBpin (a)[61] or $Cs_2CO_3$ then $PhSiH_3$ (b)[60] to regenerate the pre-catalyst phosphine. The alkyl radical (**II**) then abstracts the hydrogen atom from this phosphine to generate the cyclization product and regenerate the phosphinyl radical (Scheme 13).[60,61] Cramer *et al.* also explored using the diphosphine as the catalyst for the cyclization reactions to bypass the light activation step, which resulted in reduced yields in the dark. These results indicate the significance of the light, which can regenerate the phosphinyl radical and restore the catalytic cycle from radical chain terminations that occur before the completion of the reaction.[61]

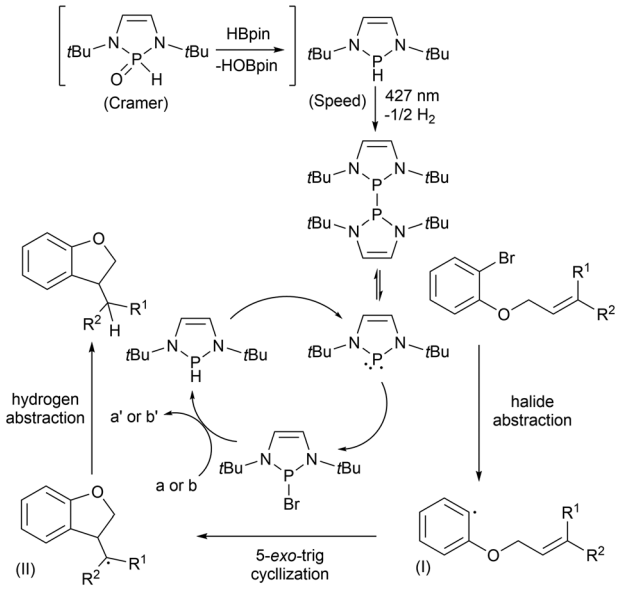


**Scheme 13** Proposed catalytic cycle of aryl halide cyclization reactions.

One of the most well-known and early developed uses of bismuth in catalysis is in the heterogeneous Standard Oil of Ohio Company (SOHIO) process. In the SOHIO process, a bismuth molybdate catalyst such as $Bi_2O_3{\cdot}MoO_3$ is involved in the rate-determining hydrogen abstraction step of the ammoxidation or oxidation of propene to give acrylonitrile or acrolein respectively.[158,159] Further application of bismuth in new catalytic radical reactions is of recent interest due to bismuth's low relative costs, non-carcinogenetic properties, low toxicity, potential recyclability, and its relativistic interaction of the large spin-orbit coupling, allowing for UV-vis transitions.[14,15,29] In 2023, Cornella *et al.* published work applying a bismuthinidene (**87**) in catalytic amounts to promote C($sp^3$)–N bond formation in a unique manner without requiring a photo-redox system, a chemical oxidant, an external base, or an electrochemical set-up; the previously necessary tools or components for the successful transformation reaction.[160] This bismuth-catalyzed cross-coupling reaction proceeds through a single-electron transfer from the Bi(I) complex **87**, with an overall Bi (I/II) or Bi(I/II/III) radical incorporating redox cycle as seen in the general Scheme 14.[160] Following a recent review focused on bismuth in radical chemistry and catalysis,[14] the area of bismuth in photocatalysis continued to expand.[161–163] In one instance, the application of stoichiometric organobismuth in photocatalytic arylations has been reported.[161] This work generated aryl radicals through the light-mediated SET of organobismuth radical cation intermediates to generate aryl radicals, which further react to obtain several arylated products.[161]

Following this work, bismuth photocatalysis has also been recently explored in a publication by Cornella and coworkers using the same bismuthinidene.[162,163] The activation and C–C coupling of aryl iodides was reported by the light-induced homolytic cleavage of bismuth–aryl bonds, generating a series

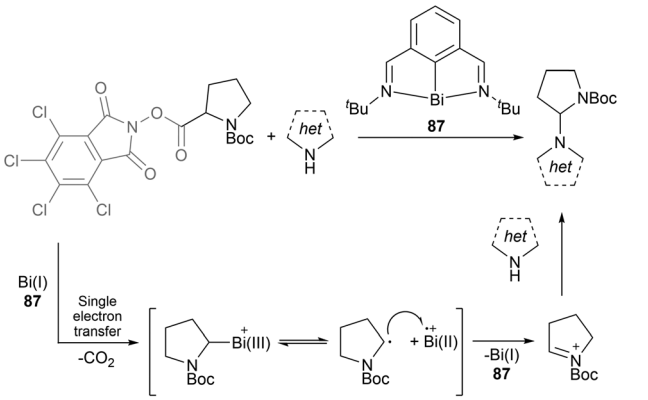


**Scheme 14** Bi(I)-catalyzed formal C($sp^3$)–N cross-coupling by radical activation of α-amino redox-active esters.

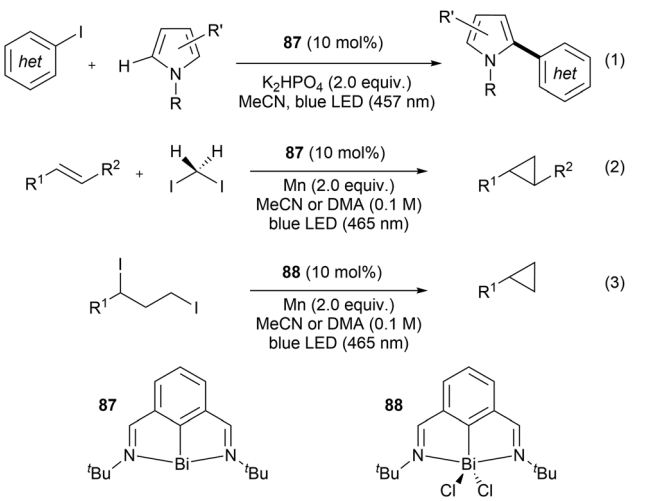


**Scheme 15** Light-induced catalytic reactions using bismuth-based catalysts.

of aryl–aryl coupling products [Scheme 15, eqn (1)].[163] The bismuth catalyst (**61**) used in this work generates a bismuth radical intermediate, where then the product and bismuth catalyst are generated and regenerated respectively by a proton-coupled electron transfer step.[163] Furthermore, using the same bismuth catalyst design (**87**, **88**), Cornella *et al.* also reported the intermolecular [Scheme 15, eqn (2)] and intramolecular [Scheme 15, eqn (3)] cyclopropanation of double bonds under light irradiation.[162] With these recent developments, the further expansion of organobismuth complexes in photocatalysis is a promising area for utilizing heavier Group 15 radicals.

Recently, multi-radical centered pnictogens have been reported to demonstrate photoswitching behaviour. The bis-biradical **89** has been reported to experience light-induced on-off switching of $H_2$ addition, where as seen in Scheme 16, the $H_2$ addition is dependent on the irradiation/housane (**89-H**) formation.[143] Furthermore, in other work reported by Schulz *et al.*, an additional cyclopentane-1,3-diyl derivative (**90**) was

 

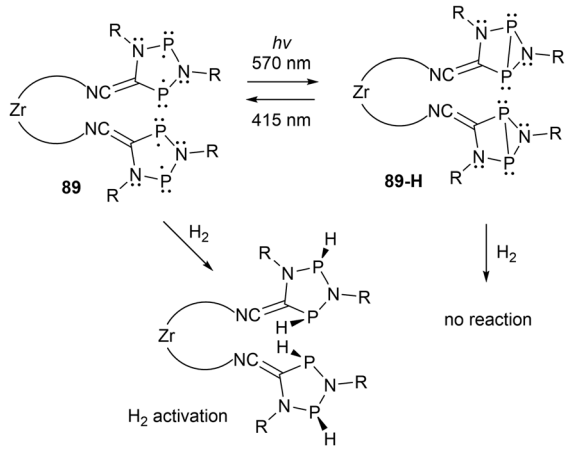


**Scheme 16** Photo-switching and $H_2$ activation investigation of tetraradical **89** and its bis(housane) **89-H**.

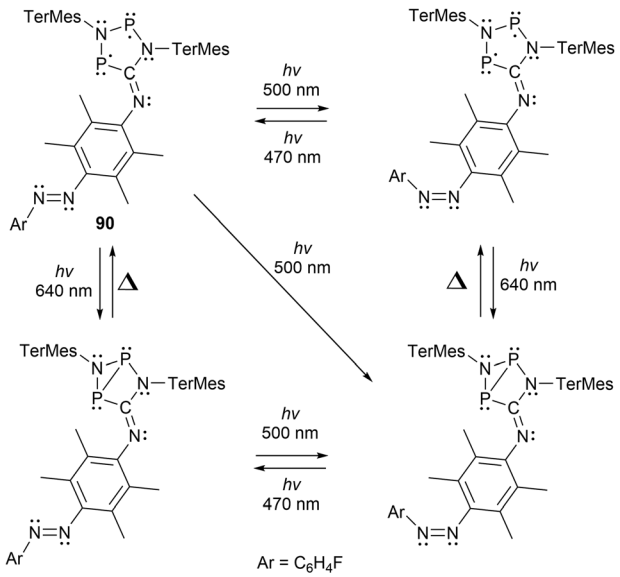


**Scheme 17** Novel molecular double switch undergoing constitutional and stereo-isomerization upon irradiation with visible light.

generated and functions as a novel molecular double switch capable of performing either a constitutional or stereo-isomerization process when irradiated with different visible light frequencies (Scheme 17).[164]

## Future implications and conclusions

Within the field of Group 15 radicals, there are potential directions this work could be directed. An area with promising potential for future work is the light-induced reactivity studies with the phosphinyl radical catalysts. Between the phosphinyl radical catalysis work done by Speed[60] and Cramer[61] as seen in Scheme 12, eqn (3) and (4), no examples of intermolecular cyclization, and only two examples of intramolecular cyclization

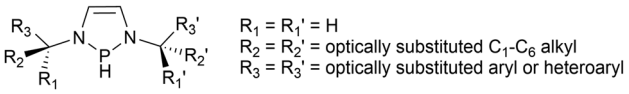


**Fig. 9** Chiral diazaphopholene framework developed by Speed.[165]

reactions using aryl chlorides were successful. Tuning the phosphinyl radical through the N–R substituents and backbone to give the desired reactivity, while still maintaining sufficient stability for ease of pre-catalyst or catalyst handling could be explored for this application. For example, the N–P–N angle could be tuned by changing the size of the heterocycle to give 6- or 7-membered ring systems to change the energies of the frontier orbitals at the P atom. Additionally, in a patent by Speed, an N-heterocyclic phosphine similar to the phosphinyl pre-catalyst used in the annulation of aryl halides[60] was used to reduce imines asymmetrically.[165] The phosphine in this case incorporates chiral alkyl substituents attached to the nitrogen atoms, promoting the enantioselectivity of the products (Fig. 9).[165] Future studies using chiral phosphinyl catalysts should be investigated for use in enantioselective catalysis.

An additional area to further develop within group 15 mono-radicals includes mixed pnictogen systems stabilized by carbenes and/or aryl substituents. The current frameworks include a variety of bi-, tri-, and tetrapnictogen-centered radicals and radical ions for nitrogen and phosphorus (Fig. 3), as well as some examples of bi- and tripnictogen nitrogen-arsenic and phosphorus-arsenic examples. Expanding this list to include examples of antimony and bismuth in these systems should be the next step. In general, the next steps should focus on developing more stable or even air-stable group 15 radical species, which can be further investigated within these processes.

Work in the area of bismuth-based radicals is expected to be a continued hot area and changes to the ligand frameworks should provide new and exciting chemistry. For example, as we were writing this conclusion, Cornella *et al.* published a red-light activated bismuthinidene where oxidative addition of aryl iodides occurs at bismuth through a SET mechanism.[166]

In addition to the wide variety of known ligands and substituent combinations available, new ligand frameworks are always being developed. We anticipate the area of heavier group 15 radicals to continue to be a hot area in main group chemistry and it is our hope that further breakthroughs will direct the area towards discoveries that will be embraced by the general chemistry community.

## Author contributions

Conceptualization, data curation, formal analysis, project administration, and writing (review/editing) was contributed by all authors. JDM contributed to funding acquisition, resources, and supervision. DLGS performed the investigation, visualization, and writing of the original draft.

## Data availability

No primary research results, software or code have been included, and no new data were generated or analyzed as part of this review.

## Conflicts of interest

There are no conflicts to declare.

## Acknowledgements

The authors thank the Natural Science and Engineering Council of Canada (NSERC) for operating funds (JDM) and the award of a Canadian Graduate Scholarship – Master's (DLGS). We also thank the reviewers for their insightful comments and suggestions.

## References

1 Z. Feng, S. Tang, Y. Su and X. Wang, *Chem. Soc. Rev.*, 2022, **51**, 5930–5973.
2 C. D. Martin, M. Soleilhavoup and G. Bertrand, *Chem. Sci.*, 2013, **4**, 3020.
3 M. Gomberg, *J. Am. Chem. Soc.*, 1900, **22**, 757–771.
4 L. N. Bochkarev, N. E. Molosnova, L. N. Zakharov, G. K. Fukin, A. I. Yanovsky and Y. T. Struchkov, *Acta Crystallogr., Sect. C:Cryst. Struct. Commun.*, 1995, **51**, 489–491.
5 P. P. Power, *Chem. Rev.*, 2003, **103**, 789–810.
6 V. V. Pen'kovskii, *Russ. Chem. Rev.*, 1975, **44**, 449–467.
7 J. P. Bullock, A. M. Bond, R. T. Boeré, T. M. Gietz, T. L. Roemmele, S. D. Seagrave, J. D. Masuda and M. Parvez, *J. Am. Chem. Soc.*, 2013, **135**, 11205–11215.
8 X. Pan, X. Chen, T. Li, Y. Li and X. Wang, *J. Am. Chem. Soc.*, 2013, **135**, 3414–3417.
9 B. Das, A. Makol and S. Kundu, *Dalton Trans.*, 2022, **51**, 12404–12426.
10 G. Tan and X. Wang, *Chin. J. Chem.*, 2018, **36**, 573–586.
11 D. Griller and K. U. Ingold, *Acc. Chem. Res.*, 1976, **9**, 13–19.
12 Y. Su and R. Kinjo, *Coord. Chem. Rev.*, 2017, **352**, 346–378.
13 C. Helling and S. Schulz, *Eur. J. Inorg. Chem.*, 2020, **2020**, 3209–3221.
14 M. Mato and J. Cornella, *Angew. Chem., Int. Ed.*, 2024, **63**, e202315046.
15 J. Ramler, I. Krummenacher and C. Lichtenberg, *Chem. – Eur. J.*, 2020, **26**, 14551–14555.
16 J. M. Lipshultz, G. Li and A. T. Radosevich, *J. Am. Chem. Soc.*, 2021, **143**, 1699–1721.
17 S. Ishida, F. Hirakawa and T. Iwamoto, *Bull. Chem. Soc. Jpn.*, 2018, **91**, 1168–1175.
18 C. Lichtenberg, in *Encyclopedia of Inorganic and Bioinorganic Chemistry*, ed. R. A. Scott, Wiley, 2nd edn, 2020, pp. 1–12.
19 N. S. Imyanitov, *Found. Chem.*, 2019, **21**, 255–284.
20 M. Seth, M. Dolg, P. Fulde and P. Schwerdtfeger, *J. Am. Chem. Soc.*, 1995, **117**, 6597–6598.
21 B. J. Dunne and A. G. Orpen, *Acta Crystallogr., Sect. C: Cryst. Struct. Commun.*, 1991, **47**, 345–347.
22 A. N. Sobolev, V. K. Belsky, N. Y. Chernikova and F. Y. Akhmadulina, *J. Organomet. Chem.*, 1983, **244**, 129–136.
23 E. A. Adams, J. W. Kolis and W. T. Pennington, *Acta Crystallogr., Sect. C:Cryst. Struct. Commun.*, 1990, **46**, 917–919.
24 L. Bučinský, D. Jayatilaka and S. Grabowsky, *J. Phys. Chem. A*, 2016, **120**, 6650–6669.
25 R. J. F. Berger, D. Rettenwander, S. Spirk, C. Wolf, M. Patzschke, M. Ertl, U. Monkowius and N. W. Mitzel, *Phys. Chem. Chem. Phys.*, 2012, **14**, 15520.
26 P. S. Bagus, Y. S. Lee and K. S. Pitzer, *Chem. Phys. Lett.*, 1975, **33**, 408–411.
27 P. Pyykko, *Chem. Rev.*, 1988, **88**, 563–594.
28 A. Kyono and M. Kimata, *Am. Mineral.*, 2004, **89**, 932–940.
29 J. Ramler, I. Krummenacher and C. Lichtenberg, *Angew. Chem., Int. Ed.*, 2019, **58**, 12924–12929.
30 K. Balasubramanian, Y. S. Chung and W. S. Glaunsinger, *J. Chem. Phys.*, 1993, **98**, 8859–8869.
31 D. Dai and K. Balasubramanian, *J. Chem. Phys.*, 1990, **93**, 1837–1846.
32 M. Kaupp, in *The Chemical Bond*, ed. G. Frenking and S. Shaik, Wiley, 1st edn, 2014, pp. 1–24.
33 Y. H. Budnikova, *Dokl. Chem.*, 2022, **507**, 229–259.
34 S. Kundu, S. Sinhababu, V. Chandrasekhar and H. W. Roesky, *Chem. Sci.*, 2019, **10**, 4727–4741.
35 A. Schulz, *Dalton Trans.*, 2018, **47**, 12827–12837.
36 G. E. Cutsail, *Dalton Trans.*, 2020, **49**, 12128–12135.
37 A. Dasgupta, E. Richards and R. L. Melen, *Angew. Chem., Int. Ed.*, 2021, **60**, 53–65.
38 L. J. C. van der Zee, S. Pahar, E. Richards, R. L. Melen and J. C. Slootweg, *Chem. Rev.*, 2023, **123**, 9653–9675.
39 S. Ishida, F. Hirakawa and T. Iwamoto, *Chem. Lett.*, 2015, **44**, 94–96.
40 F. Hirakawa, H. Ichikawa, S. Ishida and T. Iwamoto, *Organometallics*, 2015, **34**, 2714–2716.
41 N. A. Giffin, A. D. Hendsbee and J. D. Masuda, *Dalton Trans.*, 2016, **45**, 12636–12638.
42 A. Ott, P. R. Nagy and Z. Benkő, *Inorg. Chem.*, 2022, **61**, 16266–16281.
43 Y.-R. Luo, *Handbook of Bond Dissociation Energies in Organic Compounds*, CRC Press, Boca Raton, 2002.
44 C. Branfoot, T. A. Young, D. F. Wass and P. G. Pringle, *Dalton Trans.*, 2021, **50**, 7094–7104.
45 N. A. Giffin, A. D. Hendsbee, T. L. Roemmele, M. D. Lumsden, C. C. Pye and J. D. Masuda, *Inorg. Chem.*, 2012, **51**, 11837–11850.
46 M. Blum, O. Puntigam, S. Plebst, F. Ehret, J. Bender, M. Nieger and D. Gudat, *Dalton Trans.*, 2016, **45**, 1987–1997.

 

47 S. L. Hinchley, C. A. Morrison, D. W. H. Rankin, C. L. B. Macdonald, R. J. Wiacek, A. H. Cowley, M. F. Lappert, G. Gundersen, J. A. C. Clyburne and P. P. Power, *Chem. Commun.*, 2000, 2045–2046.
48 J.-D. Guo, S. Nagase and P. P. Power, *Organometallics*, 2015, **34**, 2028–2033.
49 M. J. S. Gynane, A. Hudson, M. F. Lappert and P. P. Power, *J. Chem. Soc., Chem. Commun.*, 1976, 623–624.
50 M. J. S. Gynane, A. Hudson, M. F. Lappert, P. P. Power and H. Goldwhite, *J. Chem. Soc., Dalton Trans.*, 1980, 2428–2433.
51 O. Puntigam, D. Förster, N. A. Giffin, S. Burck, J. Bender, F. Ehret, A. D. Hendsbee, M. Nieger, J. D. Masuda and D. Gudat, *Eur. J. Inorg. Chem.*, 2013, **2013**, 2041–2050.
52 S. Isenberg, S. Weller, D. Kargin, S. Valić, B. Schwederski, Z. Kelemen, C. Bruhn, K. Krekić, M. Maurer, C. M. Feil, M. Nieger, D. Gudat, L. Nyulászi and R. Pietschnig, *ChemistryOpen*, 2019, **8**, 1235–1243.
53 A. Hinz, R. Kuzora, U. Rosenthal, A. Schulz and A. Villinger, *Chem. – Eur. J.*, 2014, **20**, 14659–14673.
54 T. Taniguchi, *Synthesis*, 2017, 3511–3534.
55 S. Ishida, F. Hirakawa and T. Iwamoto, *J. Am. Chem. Soc.*, 2011, **133**, 12968–12971.
56 O. Back, M. A. Celik, G. Frenking, M. Melaimi, B. Donnadieu and G. Bertrand, *J. Am. Chem. Soc.*, 2010, **132**, 10262–10263.
57 K. Schwedtmann, S. Schulz, F. Hennersdorf, T. Strassner, E. Dmitrieva and J. J. Weigand, *Angew. Chem., Int. Ed.*, 2015, **54**, 11054–11058.
58 X. Pan, X. Wang, Y. Zhao, Y. Sui and X. Wang, *J. Am. Chem. Soc.*, 2014, **136**, 9834–9837.
59 O. Puntigam, L. Könczöl, L. Nyulászi and D. Gudat, *Angew. Chem., Int. Ed.*, 2015, **54**, 11567–11571.
60 R. D. Riley, B. S. N. Huchenski, K. L. Bamford and A. W. H. Speed, *Angew. Chem., Int. Ed.*, 2022, **61**, e202204088.
61 J. Klett, Ł. Woźniak and N. Cramer, *Angew. Chem., Int. Ed.*, 2022, **61**, e202202306.
62 J. Zhang, J.-D. Yang and J.-P. Cheng, *Chem. Sci.*, 2020, **11**, 4786–4790.
63 S. L. Hinchley, C. A. Morrison, D. W. H. Rankin, C. L. B. Macdonald, R. J. Wiacek, A. Voigt, A. H. Cowley, M. F. Lappert, G. Gundersen, J. A. C. Clyburne and P. P. Power, *J. Am. Chem. Soc.*, 2001, **123**, 9045–9053.
64 D. M. C. Ould, A. C. Rigby, L. C. Wilkins, S. J. Adams, J. A. Platts, S. J. A. Pope, E. Richards and R. L. Melen, *Organometallics*, 2018, **37**, 712–719.
65 A. Dumitrescu, V. L. Rudzevich, V. D. Romanenko, A. Mari, W. W. Schoeller, D. Bourissou and G. Bertrand, *Inorg. Chem.*, 2004, **43**, 6546–6548.
66 B. Çetinkaya, P. B. Hitchcock, M. F. Lappert, A. J. Thorne and H. Goldwhite, *J. Chem. Soc., Chem. Commun.*, 1982, 691–693.
67 J.-P. Bezombes, P. B. Hitchcock, M. F. Lappert and J. E. Nycz, *Dalton Trans.*, 2004, 499–501.
68 J. Geier, J. Harmer and H. Grützmacher, *Angew. Chem., Int. Ed.*, 2004, **43**, 4093–4097.
69 T. Sasamori, E. Mieda, N. Nagahora, K. Sato, D. Shiomi, T. Takui, Y. Hosoi, Y. Furukawa, N. Takagi, S. Nagase and N. Tokitoh, *J. Am. Chem. Soc.*, 2006, **128**, 12582–12588.
70 R. T. Boeré, A. M. Bond, S. Cronin, N. W. Duffy, P. Hazendonk, J. D. Masuda, K. Pollard, T. L. Roemmele, P. Tran and Y. Zhang, *New J. Chem.*, 2008, **32**, 214–231.
71 Y. Su, X. Zheng, X. Wang, X. Zhang, Y. Sui and X. Wang, *J. Am. Chem. Soc.*, 2014, **136**, 6251–6254.
72 A. Brückner, A. Hinz, J. B. Priebe, A. Schulz and A. Villinger, *Angew. Chem., Int. Ed.*, 2015, **54**, 7426–7430.
73 M. Yoshifuji, A. J. Arduengo III, T. A. Konovalova, L. D. Kispert, M. Kikuchi and S. Ito, *Chem. Lett.*, 2006, **35**, 1136–1137.
74 H. Cui, D. Xiao, L. Zhang, H. Ruan, Y. Fang, Y. Zhao, G. Tan, L. Zhao, G. Frenking, M. Driess and X. Wang, *Chem. Commun.*, 2020, **56**, 2167–2170.
75 X. Pan, X. Wang, Z. Zhang and X. Wang, *Dalton Trans.*, 2015, **44**, 15099–15102.
76 X. Pan, Y. Su, X. Chen, Y. Zhao, Y. Li, J. Zuo and X. Wang, *J. Am. Chem. Soc.*, 2013, **135**, 5561–5564.
77 P. Federmann, H. K. Wagner, P. W. Antoni, J.-M. Mörsdorf, J. L. Pérez Lustres, H. Wadepohl, M. Motzkus and J. Ballmann, *Org. Lett.*, 2019, **21**, 2033–2038.
78 S. Asami, S. Ishida, T. Iwamoto, K. Suzuki and M. Yamashita, *Angew. Chem., Int. Ed.*, 2017, **56**, 1658–1662.
79 G. Tan, J. Li, L. Zhang, C. Chen, Y. Zhao, X. Wang, Y. Song, Y.-Q. Zhang and M. Driess, *Angew. Chem., Int. Ed.*, 2017, **56**, 12741–12745.
80 C. Chen, Z. Hu, J. Li, H. Ruan, Y. Zhao, G. Tan, Y. Song and X. Wang, *Inorg. Chem.*, 2020, **59**, 2111–2115.
81 F. Murakami, S. Sasaki and M. Yoshifuji, *J. Am. Chem. Soc.*, 2005, **127**, 8926–8927.
82 S. Sasaki, F. Murakami and M. Yoshifuji, *Angew. Chem., Int. Ed.*, 1999, **38**, 340–343.
83 G. Tan, S. Li, S. Chen, Y. Sui, Y. Zhao and X. Wang, *J. Am. Chem. Soc.*, 2016, **138**, 6735–6738.
84 M. K. Mondal, L. Zhang, Z. Feng, S. Tang, R. Feng, Y. Zhao, G. Tan, H. Ruan and X. Wang, *Angew. Chem., Int. Ed.*, 2019, **58**, 15829–15833.
85 M. N. Hopkinson, C. Richter, M. Schedler and F. Glorius, *Nature*, 2014, **510**, 485–496.
86 J. Back, J. Park, Y. Kim, H. Kang, Y. Kim, M. J. Park, K. Kim and E. Lee, *J. Am. Chem. Soc.*, 2017, **139**, 15300–15303.
87 A. Doddi, D. Bockfeld, M.-K. Zaretzke, C. Kleeberg, T. Bannenberg and M. Tamm, *Dalton Trans.*, 2017, **46**, 15859–15864.
88 M. K. Sharma, D. Rottschäfer, S. Blomeyer, B. Neumann, H.-G. Stammler, M. Van Gastel, A. Hinz and R. S. Ghadwal, *Chem. Commun.*, 2019, **55**, 10408–10411.
89 O. Back, B. Donnadieu, P. Parameswaran, G. Frenking and G. Bertrand, *Nat. Chem.*, 2010, **2**, 369–373.

90 J. Haberstroh, C. Taube, J. Fidelius, S. Schulz, N. Israel, E. Dmitrieva, R. M. Gomila, A. Frontera, R. Wolf, K. Schwedtmann and J. J. Weigand, *Chem. Commun.*, 2024, **60**, 8537–8540.
91 E. A. LaPierre, L. K. Watanabe, B. O. Patrick, J. M. Rawson, H. M. Tuononen and I. Manners, *J. Am. Chem. Soc.*, 2023, **145**, 9223–9232.
92 E. A. LaPierre, B. O. Patrick and I. Manners, *J. Am. Chem. Soc.*, 2024, **146**, 6326–6335.
93 H. Kim and E. Lee, *Bull. Korean Chem. Soc.*, 2022, **43**, 1328–1341.
94 Y. Kim and E. Lee, *Chem. – Eur. J.*, 2018, **24**, 19110–19121.
95 Y. Song, H. Song, Y. Choi, J. Seo and E. Lee, *Chem. Commun.*, 2024, **60**, 8043–8046.
96 R. Kinjo, B. Donnadieu and G. Bertrand, *Angew. Chem., Int. Ed.*, 2010, **49**, 5930–5933.
97 O. Back, B. Donnadieu, M. Von Hopffgarten, S. Klein, R. Tonner, G. Frenking and G. Bertrand, *Chem. Sci.*, 2011, **2**, 858.
98 A. M. Tondreau, Z. Benkő, J. R. Harmer and H. Grützmacher, *Chem. Sci.*, 2014, **5**, 1545–1554.
99 Z. Li, X. Chen, D. M. Andrada, G. Frenking, Z. Benkö, Y. Li, J. R. Harmer, C.-Y. Su and H. Grützmacher, *Angew. Chem., Int. Ed.*, 2017, **56**, 5744–5749.
100 X. Chen, L. L. Liu, S. Liu, H. Grützmacher and Z. Li, *Angew. Chem., Int. Ed.*, 2020, **59**, 23830–23835.
101 R. Yadav, A. Sharma, B. Das, C. Majumder, A. Das, S. Sen and S. Kundu, *Chem. – Eur. J.*, 2024, **30**, e202401730.
102 D. Munz, *Organometallics*, 2018, **37**, 275–289.
103 E. Welz, J. Böhnke, R. D. Dewhurst, H. Braunschweig and B. Engels, *J. Am. Chem. Soc.*, 2018, **140**, 12580–12591.
104 M. Y. Abraham, Y. Wang, Y. Xie, R. J. Jr Gilliard, P. Wei, B. J. Vaccaro, M. K. Johnson, H. F. I. Schaefer, P. V. R. Schleyer and G. H. Robinson, *J. Am. Chem. Soc.*, 2013, **135**, 2486–2488.
105 T. Li, G. Tan, C. Cheng, Y. Zhao, L. Zhang and X. Wang, *Chem. Commun.*, 2018, **54**, 1493–1496.
106 K. M. Melancon, M. B. Gildner and T. W. Hudnall, *Chem. – Eur. J.*, 2018, **24**, 9264–9268.
107 Y. Fang, L. Zhang, C. Cheng, Y. Zhao, M. Abe, G. Tan and X. Wang, *Chem. – Eur. J.*, 2018, **24**, 3156–3160.
108 C. Helling and S. Schulz, *Eur. J. Inorg. Chem.*, 2020, 3209–3221.
109 A. Doddi, D. Bockfeld, M.-K. Zaretzke, T. Bannenberg and M. Tamm, *Chem. – Eur. J.*, 2019, **25**, 13119–13123.
110 K. Tsuji, Y. Fujii, S. Sasaki and M. Yoshifuji, *Chem. Lett.*, 1997, **26**, 855–856.
111 M. K. Sharma, S. Blomeyer, B. Neumann, H.-G. Stammler, A. Hinz, M. Van Gastel and R. S. Ghadwal, *Chem. Commun.*, 2020, **56**, 3575–3578.
112 J. Krüger, J. Haak, C. Wölper, G. E. I. Cutsail, G. Haberhauer and S. Schulz, *Inorg. Chem.*, 2022, **61**, 5878–5884.
113 C. Helling, C. Wölper, Y. Schulte, G. E. I. Cutsail and S. Schulz, *Inorg. Chem.*, 2019, **58**, 10323–10332.
114 S. Ishida, F. Hirakawa, K. Furukawa, K. Yoza and T. Iwamoto, *Angew. Chem., Int. Ed.*, 2014, **53**, 11172–11176.
115 C. Ganesamoorthy, C. Helling, C. Wölper, W. Frank, E. Bill, G. E. Cutsail and S. Schulz, *Nat. Commun.*, 2018, **9**, 87.
116 C. Helling, G. E. Cutsail III, H. Weinert, C. Wölper and S. Schulz, *Angew. Chem., Int. Ed.*, 2020, **59**, 7561–7568.
117 C. Helling, C. Wölper, G. E. Cutsail III, G. Haberhauer and S. Schulz, *Chem. – Eur. J.*, 2020, **26**, 13390–13399.
118 C. Lichtenberg, F. Pan, T. P. Spaniol, U. Englert and J. Okuda, *Angew. Chem., Int. Ed.*, 2012, **51**, 13011–13015.
119 D. P. Mukhopadhyay, D. Schleier, S. Wirsing, J. Ramler, D. Kaiser, E. Reusch, P. Hemberger, T. Preitschopf, I. Krummenacher, B. Engels, I. Fischer and C. Lichtenberg, *Chem. Sci.*, 2020, **11**, 7562–7568.
120 T. A. Hanna, A. L. Rieger, P. H. Rieger and X. Wang, *Inorg. Chem.*, 2002, **41**, 3590–3592.
121 H. M. Weinert, C. Wölper, J. Haak, G. E. Cutsail and S. Schulz, *Chem. Sci.*, 2021, **12**, 14024–14032.
122 J. Krüger, C. Wölper and S. Schulz, *Inorg. Chem.*, 2020, **59**, 11142–11151.
123 T. Li, H. Wei, Y. Fang, L. Wang, S. Chen, Z. Zhang, Y. Zhao, G. Tan and X. Wang, *Angew. Chem.*, 2017, **129**, 647–651.
124 R. Kretschmer, D. A. Ruiz, C. E. Moore, A. L. Rheingold and G. Bertrand, *Angew. Chem., Int. Ed.*, 2014, **53**, 8176–8179.
125 R. J. Schwamm, J. R. Harmer, M. Lein, C. M. Fitchett, S. Granville and M. P. Coles, *Angew. Chem., Int. Ed.*, 2015, **54**, 10630–10633.
126 S. Sasaki, K. Sutoh, F. Murakami and M. Yoshifuji, *J. Am. Chem. Soc.*, 2002, **124**, 14830–14831.
127 J. S. Wenger, M. Weng, G. N. George and T. C. Johnstone, *Nat. Chem.*, 2023, **15**, 633–640.
128 M. Taghavikish, B. L. Price, T. L. Roemmele and R. T. Boeré, *Aust. J. Chem.*, 2013, **66**, 1226.
129 T. Dunaj, M. Egorycheva, A. Arebi, K. Dollberg and C. von Hänisch, *Z. Anorg. Allg. Chem.*, 2023, **649**, e202300004.
130 S. Demeshko, C. Godemann, R. Kuzora, A. Schulz and A. Villinger, *Angew. Chem., Int. Ed.*, 2013, **52**, 2105–2108.
131 E. Zander, J. Bresien, V. V. Zhivonitko, J. Fessler, A. Villinger, D. Michalik and A. Schulz, *J. Am. Chem. Soc.*, 2023, **145**, 14484–14497.
132 J. Rosenboom, F. Taube, L. Teichmeier, A. Villinger, M. Reinhard, S. Demeshko, M. Bennati, J. Bresien, B. Corzilius and A. Schulz, *Angew. Chem., Int. Ed.*, 2024, **63**, e202318210.
133 H. Steffenfauseweh, Y. V. Vishnevskiy, B. Neumann, H.-G. Stammler, D. M. Andrada and R. S. Ghadwal, *Angew. Chem., Int. Ed.*, 2022, **61**, e202207415.
134 J. Bresien, A. Schulz, L. S. Szych, A. Villinger and R. Wustrack, *Dalton Trans.*, 2019, **48**, 11103–11111.
135 A. Hinz, J. Bresien, F. Breher and A. Schulz, *Chem. Rev.*, 2023, **123**, 10468–10526.
136 W. Schlenk and M. Brauns, *Ber. Dtsch. Chem. Ges.*, 1915, **48**, 661–669.

 

137 M. Goehring and D. Voigt, *Naturwissenschaften*, 1953, **40**, 482–482.
138 E. Niecke, A. Fuchs, F. Baumeister, M. Nieger and W. W. Schoeller, *Angew. Chem., Int. Ed. Engl.*, 1995, **34**, 555–557.
139 W. W. Schoeller, *Eur. J. Inorg. Chem.*, 2019, **2019**, 1495–1506.
140 T. Beweries, R. Kuzora, U. Rosenthal, A. Schulz and A. Villinger, *Angew. Chem., Int. Ed.*, 2011, **50**, 8974–8978.
141 J. Bresien, A. Hinz, A. Schulz and A. Villinger, *Dalton Trans.*, 2018, **47**, 4433–4436.
142 A. Hinz, A. Schulz and A. Villinger, *Angew. Chem., Int. Ed.*, 2015, **54**, 668–672.
143 P. Fritz, H. AlHamwi, A. Villinger, D. Michalik, J. Bresien, F. Reiß, T. Beweries and A. Schulz, *Chem. – Eur. J.*, 2024, **30**, e202402415.
144 M. Wu, H. Li, W. Chen, D. Wang, Y. He, L. Xu, S. Ye and G. Tan, *Chem*, 2023, **9**, 2573–2584.
145 Y. Pang, N. Nöthling, M. Leutzsch, L. Kang, E. Bill, M. van Gastel, E. Reijerse, R. Goddard, L. Wagner, D. SantaLucia, S. DeBeer, F. Neese and J. Cornella, *Science*, 2023, **380**, 1043–1048.
146 N. Burford, J. A. C. Clyburne and M. S. W. Chan, *Inorg. Chem.*, 1997, **36**, 3204–3206.
147 J. Zhang, J.-D. Yang and J.-P. Cheng, *Chem. Sci.*, 2020, **11**, 3672–3679.
148 S. Volodarsky, I. Malahov, D. Bawari, M. Diab, N. Malik, B. Tumanskii and R. Dobrovetsky, *Chem. Sci.*, 2022, **13**, 5957–5963.
149 N. J. Hill, G. Reeske and A. H. Cowley, *Main Group Chem.*, 2010, **9**, 5–10.
150 A. Hinz, A. Schulz and A. Villinger, *Chem. – Eur. J.*, 2014, **20**, 3913–3916.
151 S. Demeshko, C. Godemann, R. Kuzora, A. Schulz and A. Villinger, *Angew. Chem., Int. Ed.*, 2013, **52**, 2105–2108.
152 A. Hinz, A. Schulz and A. Villinger, *Angew. Chem., Int. Ed.*, 2015, **54**, 2776–2779.
153 A. Hinz, A. Schulz and A. Villinger, *J. Am. Chem. Soc.*, 2015, **137**, 9953–9962.
154 A. Hinz, A. Schulz and A. Villinger, *Chem. Sci.*, 2016, **7**, 745–751.
155 Y. Pilopp, J. Bresien, K. P. Lüdtke and A. Schulz, *Chem. – Eur. J.*, 2025, **31**, e202403893.
156 Y. Kim and Y. Lee, *Angew. Chem., Int. Ed.*, 2018, **57**, 14159–14163.
157 B. S. N. Huchenski, K. N. Robertson and A. W. H. Speed, *Eur. J. Org. Chem.*, 2020, 5140–5144.
158 T. Hanna, *Coord. Chem. Rev.*, 2004, **248**, 429–440.
159 Y. H. Jang and W. A. Goddard, *J. Phys. Chem. B*, 2002, **106**, 5997–6013.
160 M. Mato, D. Spinnato, M. Leutzsch, H. W. Moon, E. J. Reijerse and J. Cornella, *Nat. Chem.*, 2023, **15**, 1138–1145.
161 N. D. Chiappini, E. P. Geunes, E. T. Bodak and R. R. Knowles, *ACS Catal.*, 2024, **14**, 2664–2670.
162 S. Ni, D. Spinnato and J. Cornella, *J. Am. Chem. Soc.*, 2024, **146**, 22140–22144.
163 M. Mato, A. Stamoulis, P. C. Bruzzese and J. Cornella, *Angew. Chem., Int. Ed.*, 2025, **64**, e202418367.
164 Y. Pilopp, H. Beer, J. Bresien, D. Michalik, A. Villinger and A. Schulz, *Chem. Sci.*, 2025, **16**, 876–888.
165 A. W. H. Speed, *US Pat.*, 11161863, 2021.
166 A. Stamoulis, M. Mato, P. C. Bruzzese, M. Leutzsch, A. Cadranel, M. Gil-Sepulcre, F. Neese and J. Cornella, *J. Am. Chem. Soc.*, 2025, **147**, 6037–6048.